J|A|C|S

A R T I C L E S

Published on Web 03/15/2003

Mussel Adhesive Protein Mimetic Polymers for the Preparation of Nonfouling Surfaces

Jeffrey L. Dalsin, Bi-Huang Hu, Bruce P. Lee, and Phillip B. Messersmith*

Contribution from the Biomedical Engineering Department and Institute for Bioengineering and Nanoscience in Advanced Medicine, Northwestern University, Evanston, Illinois 60208

Received September 10, 2002; E-mail: philm@northwestern.edu

Abstract: A new biomimetic strategy for modification of biomaterial surfaces with poly(ethylene glycol) (PEG) was developed. The strategy exploits the adhesive characteristics of 3,4-dihydroxyphenylalanine (DOPA), an important component of mussel adhesive proteins, to anchor PEG onto surfaces, rendering the surfaces resistant to cell attachment. Linear monomethoxy-terminated PEGs were conjugated either to a single DOPA residue (**mPEG-DOPA**) or to the N-terminus of Ala-Lys-Pro-Ser-Tyr-Hyp-Hyp-Thr-DOPA-Lys (**mPEG-MAPD**), a decapeptide analogue of a protein found in *Mytilus edulis* adhesive plaques. Gold and titanium surfaces were modified by adsorption of **mPEG-DOPA** and **mPEG-MAPD** from solution, after which surface analysis by X-ray photoelectron spectroscopy and time-of-flight secondary ion mass spectroscopy confirmed the presence of immobilized PEG on the surface. The ability of modified surfaces to resist cell attachment was examined by culturing 3T3 fibroblasts on the surfaces for up to 14 days. Quantitative image analysis revealed that cell adhesion to **mPEG-DOPA** and **mPEG-MAPD** modified surfaces decreased by as much as 98% compared to control surfaces. Modified Ti surfaces exhibited low cell adhesion for up to 2 weeks in culture, indicating that the nonfouling properties of **mPEG-DOPA** and **mPEG-MAPD** treated surfaces persist for extended periods of time. This strategy paradoxically exploits the strong fouling characteristics of MAP analogues for antifouling purposes and may be broadly applied to medical implants and diagnostics, as well as numerous nonmedical applications in which the minimization of surface fouling is desired.

Introduction

The development of improved strategies for preventing molecular, cellular, and organismic fouling of surfaces is important to the future success of numerous emerging technologies. In the healthcare arena, for example, the function of therapeutic and diagnostic devices can be compromised by nonspecific adsorption of proteins and cells onto device surfaces during long-term in vivo or ex vivo exposure to physiologic fluids. While a variety of strategies have been used to control protein, cell, and bacterial adsorption at interfaces with biological tissues, one approach that has met with considerable success is surface modification with poly(ethylene glycol) (PEG),[1] a biocompatible polymer which when immobilized onto surfaces confers protein and cell resistance.[2] Existing immobilization strategies often require the presence of specific surface functional groups and extensive optimization, have a limited capacity to be used for modification of a variety of materials, and may result in immobilized PEG coatings that are susceptible to hydrolysis and/or thermal degradation.[1] Thus, there exists an ongoing need for versatile immobilization strategies that are capable of robustly anchoring PEG and other antifouling polymers onto a variety of medically relevant material surfaces.

In our efforts to develop new nonfouling materials, we have looked to an unlikely source for inspiration − mussels, one of nature's most notorious fouling organisms. Mussels, which are famous for their ability to adhere to marine surfaces, secrete protein adhesives for attachment to the substrates upon which they reside.[3] The liquid protein adhesives secreted by these organisms rapidly harden to form a solid adhesive plaque capable of mediating firm attachment to a wide variety of wet surfaces, such as rocks, metal and polymer ship hulls, and wood structures. The adhesive and cohesive properties of mussel adhesive proteins (MAPs) have been linked to the presence of L-3,4-dihydroxyphenylalanine (DOPA), a catecholic amino acid that is formed by posttranslational modification of tyrosine.[4,5] A common feature of MAPs isolated from different species of mussels is the presence of tandem repeat sequences of approximately 5−15 amino acids, of which one or more residues are DOPA.[6−9] This is exemplified by the decapeptide Ala-Lys-Pro-Ser-Tyr-DHP-Hyp-Thr-DOPA-Lys (DHP = dihydroxyproline), which is tandemly repeated some 75−85 times to make

(1) Golander, C.-G.; Herron, J. N.; Lim, K.; Claesson, P.; Stenius, P.; Andrade, J. D. In *Poly(ethylene glycol) Chemistry*; Harris, J. M., Ed.; Plenum Press: New York, 1992.
(2) Harris, J. M.; Zalipsky, S. *Poly(ethylene glycol): Chemistry and Biological Applications*; American Chemical Society: Washington, DC, 1997.
(3) Waite, J. H. *Chemtech* **1987**, *17*, 692−697.
(4) Waite, J. H.; Tanzer, M. L. *Science* **1981**, *212*, 1038−1040.
(5) Waite, J. H.; Tanzer, M. L. *Biochem. Biophys. Res. Commun.* **1980**, *96*, 1554−1561.
(6) Waite, J. H. *J. Biol. Chem.* **1983**, *258*, 2911−2915.
(7) Waite, J. H.; Housley, T. J.; Tanzer, M. L. *Biochemistry* **1985**, *24*, 5010−5014.
(8) Laursen, R. A. In *Structure, Cellular Synthesis and Assembly of Biopolymers*; Case, S. T., Ed.; Springer-Verlag: Berlin, 1992; pp 55−74.
(9) Yamamoto, H. *Biotechnol. Genet. Eng. Rev.* **1996**, *13*, 133−165.

Chart 1. Biomimetic PEG Conjugates Used for Surface Modification

n̄ = 45   mPEG-DOPA 2k

n̄ = 113 mPEG-DOPA 5k

n̄ = 45   mPEG-MAPD 2k

n̄ = 113 mPEG-MAPD 5k
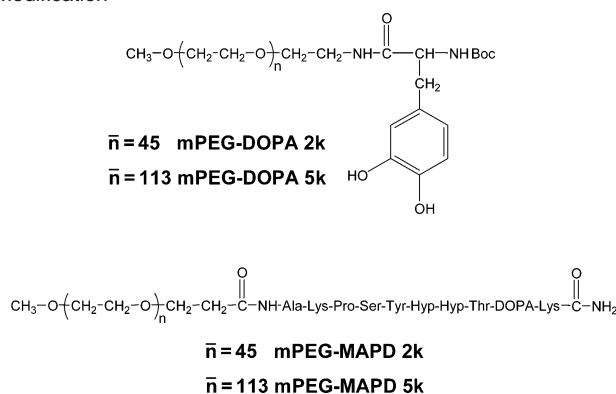
up the majority of the *Mytilus edulis* foot protein 1 (Mefp1).[6,10] Although the exact mechanism of MAP adhesion to surfaces is not fully understood, it has been widely speculated as being due in part to chemical interactions between the catechol side chain of DOPA residues and the surfaces to which the protein is adsorbed.[11,12]

Although numerous attempts have been made to incorporate DOPA into synthetic polymers in an effort to develop novel adhesive materials,[13–19] the use of DOPA-containing polymers for the preparation of nonadhesive/nonfouling surfaces has not been previously explored. In this paper, we exploit the strong fouling characteristics of MAP analogues for antifouling purposes by designing DOPA-containing peptide-PEG conjugates, reasoning that DOPA-containing peptides would provide robust and versatile anchors for the immobilization of antifouling polymers onto metal, metal oxide, and polymer surfaces. Electron and mass spectroscopic evidence established the immobilization of DOPA-functionalized PEGs onto gold and titanium surfaces, and cell culture experiments demonstrated the resistance of these surfaces to cell attachment.

Results and Discussion

We synthesized several linear conjugates of PEG and DOPA-containing peptides (Chart 1). The simplest constructs, **mPEG-DOPA 2k** and **mPEG-DOPA 5k**, consisted of a single *N*-Boc-DOPA amino acid conjugated to the end of a methoxy-terminated PEG of molecular weight 2 or 5 kDa.[19] More sophisticated constructs, **mPEG-MAPD 2k** and **mPEG-MAPD 5k**, were obtained by solid-phase synthesis of an analogue of Mefp1 decapeptide,[20] Ala-Lys-Pro-Ser-Tyr-Hyp-Hyp-Thr-DOPA-

(10) Taylor, S. W.; Waite, J. H.; Ross, M. M.; Shabanowitz, J.; Hunt, D. F. *J. Am. Chem. Soc.* **1994**, *116*, 10803−10804.
(11) Yu, M.; Hwang, J.; Deming, T. J. *J. Am. Chem. Soc.* **1999**, *121*, 5825−5826.
(12) Ooka, A.; Garrell, R. L. *Biopolymers* **2000**, *57*, 92−102.
(13) Yamamoto, H.; Ogawa, T.; Nishida, A. *J. Colloid Interface Sci.* **1995**, *176*, 105−110.
(14) Berenbaum, M. B.; Williams, J. I.; Bhattacharjee, H. R.; Goldberg, I.; Swerdloff, M. D.; Salerno, A. J.; Unger, P. D. *Polym. Prepr.* **1989**, *30*, 350−351.
(15) Swerdloff, M. D.; Anderson, S. B.; Sedgwick, R. D.; Gabriel, M. K.; Brambilla, R. J.; Hindenlang, D. M.; Williams, J. I. *Int. J. Pept. Protein Res.* **1989**, *33*, 318−327.
(16) Yu, M.; Deming, T. J. *Macromolecules* **1998**, *31*, 4739−4745.
(17) Yamada, K.; Chen, T.; Kumar, G.; Vesnovsky, O.; Topoleski, L. D. T.; Payne, G. F. *Biomacromolecules* **2000**, *1*, 252−258.
(18) Huang, K.; Lee, B.; Ingram, D.; Messersmith, P. *Biomacromolecules* **2002**, *3*, 397−406.
(19) Lee, B. P.; Dalsin, J. L.; Messersmith, P. B. *Biomacromolecules* **2002**, *3*, 1038−1047.
(20) Hu, B. H.; Messersmith, P. B. *Tetrahedron Lett.* **2000**, *41*, 5795−5798.
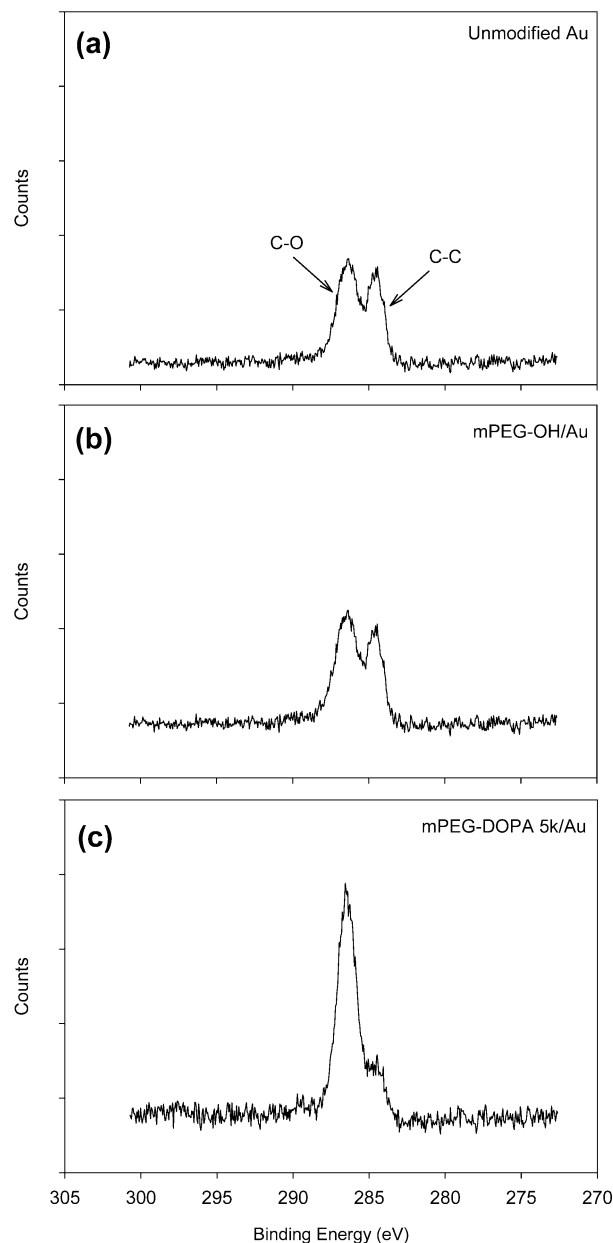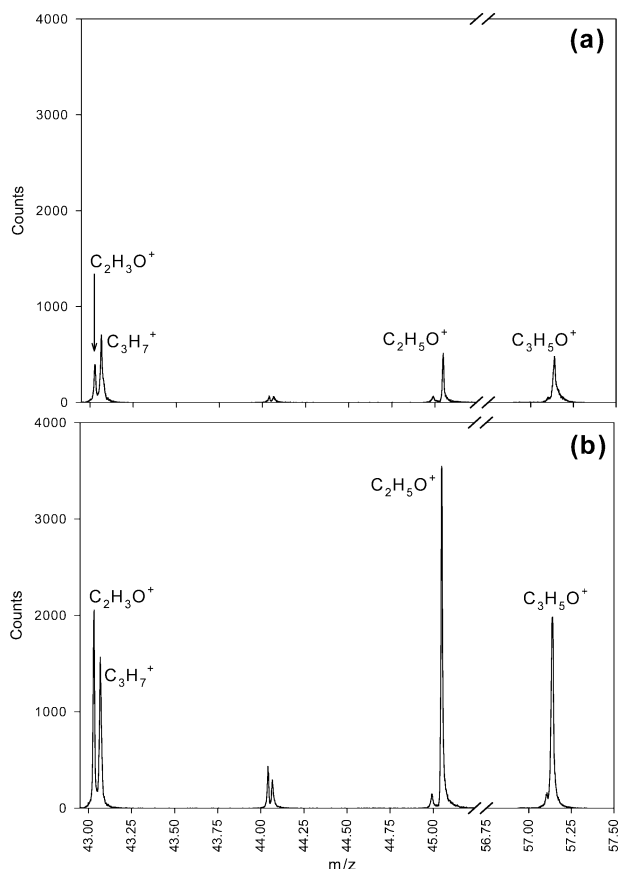
Figure 1. High-resolution C(1s) XPS spectra of (a) unmodified, (b) m-PEG-OH treated, and (c) **mPEG-DOPA 5k** treated Au substrates. A dramatic increase in the ether peak at 286.0 eV in (c) suggests the presence of PEG.

Lys, followed by on-resin coupling to a 2 or 5 kDa methoxy-terminated PEG. Products were characterized by NMR spectroscopy and mass spectroscopy and were analyzed for DOPA content. Modification of Au and Ti surfaces was performed by simple adsorption of polymer from an aqueous or organic solution.

Unmodified and PEG modified Au surfaces were initially analyzed by X-ray photoelectron spectroscopy (XPS) and time-of-flight secondary ion mass spectrometry (TOF-SIMS) analysis. XPS spectra of **mPEG-DOPA 5k** treated surfaces (Figure 1) revealed a significant increase in the ether (C−O) peak at 286.0 eV, which was not observed in control samples treated identically with a hydroxyl terminated methoxy-PEG (mPEG-OH). A smaller peak observed at 284.6 eV was attributed to the aliphatic and aromatic carbons in the PEG and DOPA headgroup, as well as some hydrocarbon contamination resulting from the preparation/evacuation process. Together, the 286.0

Figure 2. Low mass region of the positive ion TOF-SIMS spectra of (a) Au modified with mPEG-OH and (b) Au modified with **mPEG-DOPA 5k**, showing increased presence of fragments corresponding to PEG adsorption.

Figure 3. The high mass positive ion TOF-SIMS spectrum of Au substrate modified with **mPEG-DOPA 5k**, showing Au-catechol fragments ($AuOC^+$, $AuOCCO^+$, and $AuO_2C_6H_5^+$) and Au-DOPA-PEG fragments arising from immobilization of PEG by Au−DOPA interactions. Fragments representing the complexation of Au to the DOPA catechol side chain were observed at $m/z \approx 225$ ($AuOC^+$), 253 ($AuOCCO^+$), and 306 ($AuO_2C_6H_5^+$). Less intense AuO_aC_b peaks are seen at $m/z \approx 434$, 450, 462, and 478. The periodic triplets seen in the high mass range (>500 amu, see inset) correspond to Au-DOPA-$(CH_2CH_2O)_n$ fragments, where each triplet is separated by 44 amu, representing the repeat unit of the PEG chain.

eV and 284.6 eV peaks had an appearance that is typical of a surface-bound PEG polymer.[21,22]

The positive ion TOF-SIMS spectrum of unmodified Au exhibited $(C_nH_{2n+1})^+$ and $(C_nH_{2n-1})^+$ peaks typical of hydrocarbon contamination, as well as a Au peak at $m/z \approx 196.9$ (data not shown). Modification of Au surfaces with mPEG OH resulted in only modest increases in the peaks representing $C_aH_bO_c^+$ PEG fragments (Figure 2A); however, the relative abundance of $C_2H_3O^+$ ($m/z \approx 43.04$), $C_2H_5O^+$ ($m/z \approx 45.06$), and $C_3H_5O^+$ ($m/z \approx 57.07$) increased dramatically in surfaces modified with **mPEG-DOPA 5k** (Figure 2B). There was also a significant increase in the relative abundance of $C_3H_7^+$ ($m/z \approx 43.09$), which may be attributed to the fragmentation of the *tert*-butyl in the Boc protection group. In the high mass range, several notable features of the TOF-SIMS spectrum (Figure 3) suggested the presence of immobilized **mPEG-DOPA 5k**. First, the presence of peaks at m/z values of 225, 253, and 306 corresponding to $AuOC^+$, $AuO_2C_2^+$, and $AuO_2C_6H_5^+$ fragments, respectively, indicates the existence of Au-DOPA complexes. A notable feature found only in the positive ion spectrum of the **mPEG-DOPA 5k** treated Au substrate was a pattern of triplet repeats in the high mass range. Similar features have been found by other investigators in the spectra of PEGylated
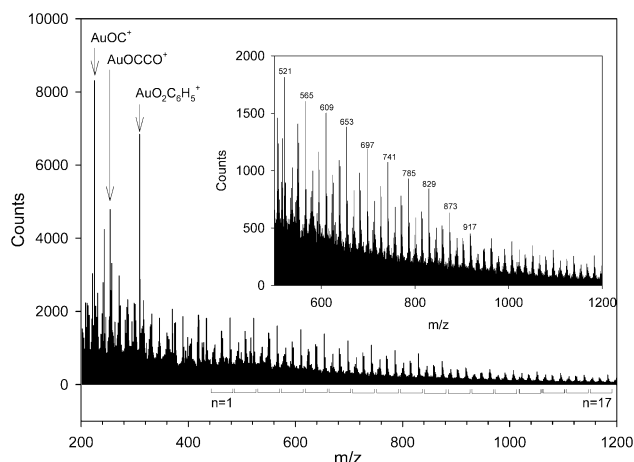
surfaces,[21,22] and in this case the mass of the triplet clusters corresponds to Au-DOPA-$(CH_2CH_2O)_n$ fragments. When further resolved (inset, Figure 3), it can be seen that each triplet cluster is separated by 44 amu, the molecular weight of the ethylene oxide repeat unit of PEG. This pattern of triplet clusters was identifiable for fragments of up to 17 repeat units, beyond which the signal was below detectable limits. Although we cannot rule out the complexation of neutral PEG fragments by Au cations in the vapor phase of the spectrometer,[23] the data suggest the anchoring of PEG onto the metal surface via direct Au−DOPA bonds. Such an interpretation is consistent with the results of Ooka and Garrell,[12] who found spectroscopic evidence for the formation of Au−catechol bonds when DOPA-containing peptides were adsorbed onto the surface of colloidal Au particles.

When fibroblasts were cultured for 4 h in the presence of modified Au surfaces, cell attachment and spreading were strongly dependent on the nature of the endgroup chemistry of the PEG chain (Figure 4). While cells readily attached and spread onto unmodified as well as mPEG-OH treated Au surfaces, the surfaces modified with DOPA-containing anchoring groups displayed significantly less cellular adhesion and spreading than the unmodified surfaces ($p < 0.05$). While the reduction in cell attachment and spreading was statistically significant for the substrates modified with **mPEG-DOPA 2k** and **mPEG-DOPA 5k** ($>56\%$ reduction in cell area for 2k PEG; $>60\%$ reduction for 5k), it was particularly dramatic for the **mPEG-MAPD 2k** and **mPEG-MAPD 5k** modified surfaces. In fact, the **mPEG-MAPD 5k** modified surface exhibited a $>98\%$ reduction in total projected cellular area as compared to unmodified gold ($p < 0.01$). Fluorescence microscopy images of **mPEG-MAPD 5k** treated Au surfaces after 4 h of exposure to cells revealed the virtual absence of attached cells as shown in Figure 5. For the substrate shown in Figure 5, only a small

(21) Moulder, J. F.; Chastain, J. *Handbook of X-ray Photoelectron Spectroscopy: A Reference Book of Standard Spectra for Identification and Interpretation of XPS Data*; Physical Electronics Division Perkin-Elmer Corp.: Eden Prairie, MN, 1992.
(22) Lu, H. B.; Campbell, C. T.; Castner, D. G. *Langmuir* **2000**, *16*, 1711−1718.
(23) Michel, R.; Luginbuhl, R.; Graham, D. J.; Ratner, B. D. *Langmuir* **2000**, *16*, 6503−6509.
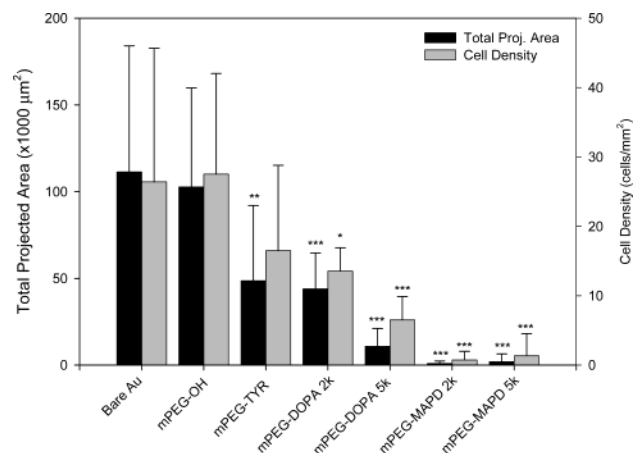
Figure 4. Comparison of total projected area and density of cell attachment and spreading of 3T3 fibroblasts after 4 h culture on Au, mPEG-OH-treated Au, **mPEG-Tyr**-treated Au, Au modified with **mPEG-DOPA**, and Au modified with **mPEG-MAPD** (*, $p < 0.05$; **, $p < 0.01$; ***, $p < 0.001$ versus bare Au).
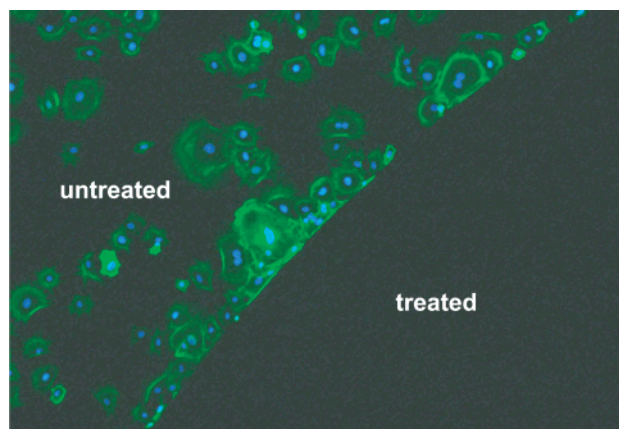

Figure 5. Fluorescence microscopy image of fibroblast attachment (4 h) to a Au substrate in which a circular portion of the surface was modified with **mPEG-MAPD 5k** (treated). The remainder of the Au surface was unmodified (untreated).

circular portion of the surface was modified by **mPEG-MAPD 5k**, after which cells readily attached to the unmodified portion of the substrate, but not the area modified by **mPEG-MAPD 5k**. More sophisticated approaches to selective area modification (e.g., microcontact printing) with these polymers could be employed for preparation of surfaces patterned with adhesive and nonadhesive regions.

DOPA-containing PEGs also confer excellent cell resistance characteristics to Ti surfaces (Figure 6). Both **mPEG-DOPA 5k** and **mPEG-MAPD 5k** modified surfaces showed significant decreases ($p < 0.001$) in 4 h cell attachment when compared to unmodified, mPEG-OH, mPEG-Phe, and mPEG-Tyr modified Ti substrates. Figure 7 displays the results of an extended cell adhesion and spreading experiment on Ti. Ti surfaces modified with **mPEG-DOPA 5k** and **mPEG-MAPD 5k** continue to resist fibroblast adhesion at 14 days, while control substrates have reached confluent monolayers. In this experiment, fresh cells were seeded twice weekly, providing a rigorous test of the ability of these surfaces to resist cell attachment over a longer period of time. The fact that cell attachment remained low throughout this experiment suggests that the nonfouling characteristics of **mPEG-DOPA 5k** and **mPEG-MAPD 5k** treated Ti surfaces may persist for extended periods of time.
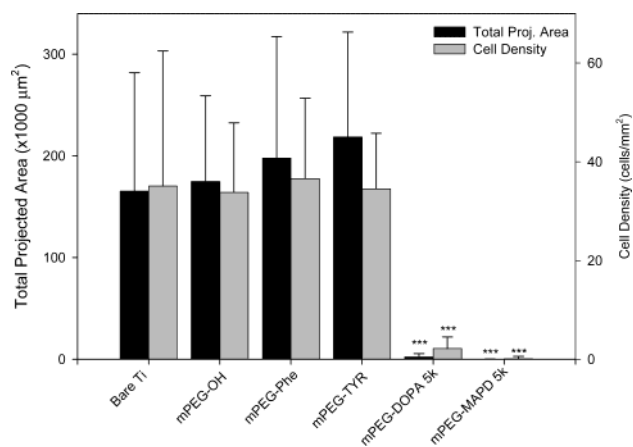
Figure 6. Comparison of total projected area and density of cell attachment and spreading of 3T3 fibroblasts after 4 h culture on Ti and Ti modified with mPEG-OH, **mPEG-Phe**, **mPEG-Tyr**, **mPEG-DOPA 5k**, and **mPEG-MAPD 5k** (***, $p < 0.001$ versus bare Ti).
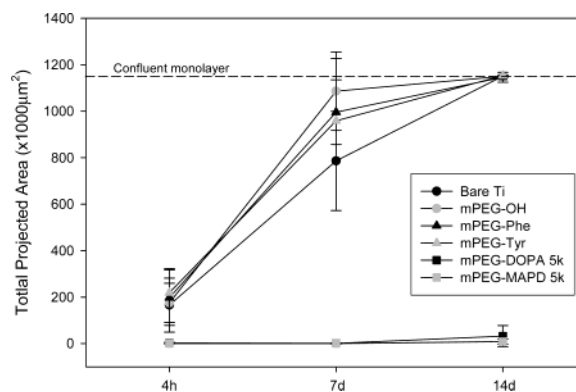

Figure 7. Long-term resistance to cell adhesion on Ti, and Ti modified with mPEG-OH, **mPEG-Phe**, **mPEG-Tyr**, **mPEG-DOPA 5k**, and **mPEG-MAPD 5k**.

It is important to note that, unlike Au, the bulk Ti substrates used in this study possess a native oxide surface. While the exact nature of the chemical interactions between the DOPA-containing PEG and the Ti substrate is still under investigation, the literature suggests that catechols form very strong surface complexes at the anatase(TiO_2)/aqueous solution interface.[24] It is likely that similar surface complexation is involved in the immobilization of DOPA modified PEG onto the Ti substrates used in this study.

It is well known that surfaces containing adsorbed MAP are highly adhesive to cells under similar conditions,[25–27] and our own control experiments performed on Au surfaces modified by Mefp1 decapeptide analogue Ala-Lys-Pro-Ser-Tyr-Hyp-Hyp-Thr-DOPA-Lys confirm this observation (data not shown). Therefore, the antifouling properties of surfaces modified with **mPEG-DOPA 5k** and **mPEG-MAPD 5k** can likely be attributed to the physical characteristics of the adsorbed polymer, in which the DOPA-containing peptide moieties strongly anchor the PEG onto the surface, while the immobilized PEG chains provide steric repulsion of protein and cell adsorption.

(24) Rodriguez, R.; Blesa, M. A.; Regazzoni, A. E. *J. Colloid Interface Sci.* **1996**, *177*, 122−131.
(25) Arnoult, C.; Cardullo, R. A.; Lemos, J. R.; Florman, H. M. *Proc. Natl. Acad. Sci. U.S.A.* **1996**, *93*, 13004−13009.
(26) Schedlich, L. J.; Young, T. F.; Firth, S. M.; Baxter, R. C. *J. Biol. Chem.* **1998**, *273*, 18347−18352.
(27) Shao, J. Y.; Ting-Beall, H. P.; Hochmuth, R. M. *Proc. Natl. Acad. Sci. U.S.A.* **1998**, *95*, 6797−6802.

Although indirect, the cell attachment results do provide some information regarding MAP processing, the relative adhesive contributions of DOPA and other MAP residues, and the adhesive performance of DOPA-containing polymers on different material surfaces. For example, a comparison of cell attachment on surfaces modified with **mPEG-DOPA** and **mPEG-Tyr** may yield clues as to the adhesive significance of the posttranslational modification reaction that converts Tyr into DOPA residues during MAP processing. In this context, it is interesting to note that cell attachment to **mPEG-DOPA 5k** modified Ti surfaces was substantially lower than **mPEG-Tyr** modified Ti at all time points, suggesting that the catechol side chain of DOPA is significantly more effective as an anchor than the phenol side chain of Tyr. However, this was not the case on Au surfaces, as 4 h cell attachment to **mPEG-DOPA 5k** modified Au was significantly less than that on unmodified Au, but not statistically different than **mPEG-Tyr** modified Au. Thus, a single DOPA residue appears to be sufficient for immobilization of PEG onto Ti surfaces, but less effective for immobilization onto Au, where exceptionally low cell attachment was only observed for surfaces modified by **mPEG-MAPD 2k** or **mPEG-MAPD 5k**. This result therefore suggests that other residues in the Mefp1 decapeptide analogue make important adhesive contributions on Au. Additional experiments are in progress to more fully explore the adhesive contributions of non-DOPA residues found in MAP consensus repeat sequences.

Conclusions

We have demonstrated the use of natural adhesive protein mimics to anchor antifouling polymers onto biomaterial surfaces. DOPA-containing peptides conjugated to PEG readily adsorb onto Au and Ti surfaces, rendering these surfaces resistant to cell attachment for up to 2 weeks. This strategy may be employed in practical situations where control of the fluid/solid interface is of essential importance. Examples of such applications include the design of cell and protein resistant surfaces desired for implantable medical implants and diagnostics, anti-icing coatings on aircraft wings, and nonfouling marine surfaces. Indeed, it is conceivable that these results may lead to novel strategies for preventing mussels and barnacles from attaching to ship hulls, piers, and other man-made structures.

Experimental Section

Materials. Monomethoxy-PEG-amine (mPEG-NH$_2$, $\bar{M}_w$ = 2k, 5k), mPEG-OH ($\bar{M}_w$ = 5k), and succinimidyl propionate activated PEG (mPEG-SPA, $\bar{M}_w$ = 2k, 5k) were purchased from Shearwater Polymers, Inc. and used as received. Rink resin (0.6 mmol/g), Fmoc-Ala, Fmoc-Lys(Boc), Fmoc-Pro, Fmoc-L-Ser(*tert*-butyl), Fmoc-Tyr(*tert*-butyl), Fmoc-Hyp, Fmoc-Thr(*tert*-butyl), BOP, HOBt, DIEA, HBTU, NMP, *N*-Boc-L-Tyr, and *N*-Boc-L-Phe were purchased from Advanced ChemTech, KY. Fmoc-DOPA(Ceof) was synthesized as described.[20] Piperidine, water (HPLC grade), EDT, thioanisole, and *m*-cresol were from Aldrich. Acetonitrile was from Burdick and Jackson. TFA was from J. T. Baker. Sephadex LH-20 was obtained from Fluka (Milwaukee, WI). L-Dopa was purchased from Lancaster (Windham, NH). *N*-Boc-L-DOPA dicyclohexylammonium salt was purchased from Sigma Chemical Co. (St. Louis, MO). Triethylamine (Et$_3$N), sodium molybdate dihydrate, and sodium nitrite were purchased from Aldrich Chemical Co. (Milwaukee, WI).

Synthesis of mPEG-MAPD. An analogue of the decapeptide consensus repeat of Mefp1, Ala-Lys-Pro-Ser-Tyr-Hyp-Hyp-Thr-DOPA-Lys, was synthesized manually on Rink resin (0.6 mmol/g with Fmoc) by Fmoc strategy. Fmoc deprotection was performed in 25% piperidine in *N*-methyl-2-pyrrolidinone (NMP) for 20 min. Coupling reactions were performed using 2 equiv of the mixture Fmoc-amino acid:BOP: HOBt:DIEA (1:1:1:1) in NMP, with a 10-min preactivation step before coupling. The coupling time was 20 min, and the reaction was monitored by the ninhydrin test. After the assembly of Mefp1 decapeptide analogue, 100 mg of the peptide-resin was cleaved using 1 M TMSBr in TFA with EDT, thioanisole, and *m*-cresol at 0 °C for 60 min. Successful synthesis of the decapeptide was confirmed by analytical RP-HPLC on the crude peptide using a Waters HPLC system (Waters, Milford, MA) on a Vydac 218TP reverse phase column (250 × 4.6 mm, 10 mm) with a gradient of acetonitrile in 0.1% TFA (v/v) water, flow rate 1 mL/min, and detection at UV 215 nm. RP-HPLC purification was performed using the same Waters HPLC system on a Vydac 218TP reverse phase column (250 × 22 mm, 10 mm) with a gradient of acetonitrile in 0.1% TFA (v/v) water, flow rate 8 mL/min, and detection at UV 215 nm. ESI-MS analysis of the purified Mefp1 peptide was performed on a LCQ LC-MS system (Finnigan, Thermoquest, CA).

The remaining Mefp1 decapeptide-resin was then coupled with **mPEG-SPA 2k** and **5k** using the coupling protocol described above. The polymer conjugates were cleaved from the resin by treatment with 1 M TMSBr in TFA in the presence of scavengers using the method described above, purified by RP-HPLC, and characterized by MALDI-MS performed on a Voyager-DE Pro system (PerSeptive Biosystem, MA). α-Cyano-4-hydroxycinnamic acid was used as a matrix.

Synthesis of mPEG-DOPA. mPEG-NH$_2$ (2.0 g, 0.40 mmol), *N*-Boc-L-DOPA dicyclohexylammonium salt (0.80 mmol), HOBt (1.3 mmol), and Et$_3$N (1.3 mmol) were dissolved in 20 mL of a 50:50 mixture of DCM and DMF. HBTU (0.80 mmol) in 10 mL of DCM was then added, and the reaction was carried out under argon at room temperature for 30 min. The reaction solution was successively washed with saturated sodium chloride solution, 5% NaHCO$_3$, diluted HCl solution, and distilled water. The crude product was concentrated under reduced pressure and purified by column chromatography on Sephadex LH-20 with methanol as the mobile phase. The product was further purified by precipitation in cold methanol three times, dried in a vacuum at room temperature, and stored under nitrogen at −20 °C.

DOPA content was determined colorimetrically using the method of Waite and Benedict.[28] Briefly, mPEG-DOPA aqueous solutions were treated with nitrite reagent (1.45 M sodium nitrite and 0.41 M sodium molybdate dihydrate) followed by the addition of excess NaOH solution. The absorbance (500 nm) of the mixture was recorded using a Hitachi U-2010 UV/vis spectrophotometer, within 2−4 min of NaOH addition. A standard curve was constructed using solutions of known DOPA concentration. ^{1}H NMR (500 MHz, CDCl$_3$/TMS): δ 6.81−6.60 (m, 3H, C$_6$H$_3$(OH)$_2$−), 6.01 (br, s, 1H, OH−), 5.32 (br, s, 1H, OH−), 4.22 (br, s, 1H, C$_6$H$_3$(OH)$_2$−CH$_2$−C*H*(N−)−C(O)N−), 3.73−3.38 (m, PEO), 3.07 (m, 2H, PEO−C*H*$_2$−NH−C(O)−), 2.73 (t, 2H, C$_6$H$_3$(OH)$_2$−C*H*$_2$−CH(N−)−C(O)N−), 1.44 (s, 9H, (CH$_3$)$_3$C−), 1.25 (s, 3H, C*H*$_3$CH$_2$O−).

Synthesis of mPEG-Phe and mPEG-Tyr. mPEG-Phe and **mPEG-Tyr** conjugates were prepared from *N*-Boc-L-Phe and *N*-Boc-L-Tyr, respectively, using mPEG-NH$_2$ (5k) and the synthesis and purification method described above for **mPEG-DOPA**. ^{1}H NMR (500 MHz, D$_2$O/TMS) for **mPEG-Phe**: δ 7.35 (m, 5H, C$_6$H$_5$−CH$_2$−), 4.28 (t, 1H, C$_6$H$_5$−CH$_2$−C*H*(N−)−C(O)N−), 3.30−3.85 (m, PEO), 3.02 (m, 2H, C$_6$H$_5$−C*H*$_2$−CH(N−)−C(O)N−), 1.37 (s, 9H, (C*H*$_3$)$_3$C−). ^{1}H NMR (500 MHz, D$_2$O/TMS) for **mPEG-Tyr**: δ 7.16 (d, 2H, C$_6$H$_2$*H*$_2$(OH)−), 6.86 (d, 2H, C$_6$H$_2$*H*$_2$(OH)−), 4.21 (t, 1H, C$_6$H$_4$(OH)−CH$_2$−C*H*(N−)−C(O)N−), 3.30−3.85 (m, PEO), 2.93 (m, 2H, C$_6$H$_4$(OH)−C*H*$_2$−CH(N−)−C(O)N−), 1.43 (s, 3H, C*H*$_3$CH$_2$O−), 1.38 (s, 9H, (C*H*$_3$)$_3$C−).

(28) Waite, J. H.; Benedict, C. V. *Methods Enzymol.* **1984**, *107*, 397−413.

Substrate Preparation. To create pristine gold surfaces, we cleaned glass coverslips (12 mm diam) by immersing them in 5% Contrad 70 solution (Decon Labs, Inc.) in an ultrasonic bath for 20 min, rinsing with MeOH, sonicating in MeOH for 20 min, rinsing in acetone, sonicating in acetone for 20 min, rinsing in petroleum ether, and sonicating in petroleum ether for 20 min. The glass surfaces were further cleaned by exposure to O_2 plasma for 5 min, after which 2 nm Cr followed by 10 nm Au (99.9% pure) were sputtered (Cressington 208HR).[22] Titanium disks (12.7 mm diam by 1 mm thick) were cut from Grade 4 Ti rodstock and polished, ultimately finishing with 0.04 μm colloidal silica. Ti disks were then ultrasonically cleaned as described above, followed by exposure to O_2 plasma for 5 min. XPS survey scans of the clean Ti substrates revealed dominant peaks at 458 eV (Ti2p) and 530 eV (O1s), confirming the presence of a native titanium oxide layer.

Surface Modification. For surface analysis by XPS and TOF-SIMS, clean substrate samples were modified in DCM (50 mg/mL) at 25 °C for 24 h. Upon removal from solution, substrates were extensively rinsed in DCM to remove unbound PEG, dried in a stream of N_2, and immediately analyzed. For cell culture experiments, clean substrates were modified by incubation in mPEG solutions (1.0 mg/mL) at 50 °C for 24 h, after which they were extensively rinsed in DI water to remove unbound PEG. Adsorption of **mPEG-DOPA**, **-Tyr**, **-Phe**, and **-OH** was performed in 0.1 M MOPS buffer (pH = 6.0) containing 0.6 M K_2SO_4, while **mPEG-MAPD** was adsorbed from a saturated NaCl solution containing 0.1 M MOPS buffer (pH = 6.0).

Surface Characterization. XPS data were collected on an Omicron ESCALAB (Omicron, Taunusstein, Germany) configured with a monochromated Al Kα (1486.8 eV) 300-W X-ray source, 1.5 mm circular spot size, a flood gun to counter charging effects, and an ultrahigh vacuum ($<10^{-8}$ Torr). The takeoff angle, defined as the angle between the substrate normal and the detector, was fixed at 45°. Substrates were mounted on standard sample studs by means of double-sided adhesive tapes. All binding energies were calibrated using either the Au(4f$_{7/2}$) peak (84.0 eV) or the C(1s) carbon peak (284.6 eV). Analysis consisted of a broad survey scan (50.0 eV pass energy) and a 10-min high-resolution scan (22.0 eV pass energy) at 270−300 eV for C(1s). Secondary ion spectra were collected on a TRIFT III time-of-flight secondary ion mass spectrometer (Physical Electronics, Eden Prairie, MN) in the mass range 0−2000 m/z. A Ga$^+$-source was used at a beam energy of 15 keV with a 100 μm raster size. Both positive and negative spectra were collected and calibrated with a set of low mass ions using the PHI software Cadence.

Cell Culture. 3T3-Swiss albino fibroblasts obtained from ATCC (Manassas, VA) were maintained at 37 °C and 10% CO_2 in Dulbecco's modified Eagle's medium (DMEM; Cellgro, Herndon, VA) containing 10% fetal bovine serum (FBS) and 100 μg/mL of penicillin and 100 U/mL of streptomycin. Immediately before use, fibroblasts of passage 12−16 were harvested using 0.25% trypsin-EDTA, resuspended in DMEM with 10% FBS, and counted using a hemocytometer.

Quantification of Cell Adhesion. Substrates were pretreated in 12-well TCPS plates with 1.0 mL of DMEM containing FBS for 30 min at 37 °C and 10% CO_2. Cells were seeded onto the substrates at a density of 2.9×10^3 cells/cm^2 and maintained in DMEM with 10% FBS at 37 °C and 10% CO_2. For long-term studies, substrates were reseeded with 2.9×10^3 cells/cm^2 twice per week. At periodic intervals, nonadherent cells were removed by aspirating the medium in each well. On Au substrates, adherent cells were fixed in 3.7% paraformaldehyde for 5 min and subsequently stained with 5 μM 1,1'-dioctadecyl-3,3,3',3'-tetramethylindocarbocyanine perchlorate (DiI; Molecular Probes, Eugene, OR) in DMSO for 30 min at 37 °C. Cells on Ti substrates were stained with 2.5 μM calcein-AM (Molecular Probes) in complete PBS for 1 h at 37 °C.

Quantitative cell attachment data were obtained by acquiring five color images from random locations on each substrate using an Olympus BX-40 (λ_{Ex} = 549 nm, λ_{Em} = 565 nm) and a Coolsnap CCD camera (Roper Scientific, Trenton, NJ). These experiments were performed in triplicate for statistical purposes, resulting in a total of 15 images per time point for each substrate. The resulting images were quantified using thresholding in Metamorph (Universal Imaging, Downington, PA). A one-way ANOVA and Tukey's post-hoc test with 95% confidence intervals (SPSS, Chicago, IL) were used to determine statistical significance of the data. The mean and standard deviation of the measurements were reported.

Supporting Information Available: Analytical HPLC and ESI-MS spectrum of decapeptide; MALDI-MS spectrum of **mPEG-MAPD 2k** and **mPEG-MAPD 5k** (PDF). This material is available free of charge via the Internet at http://pubs.acs.org.

JA0284963